

## NUMERICAL STUDY OF WICK HEAT PIPE PERFORMANCE WITH ALTERNATIVE MATERIALS IN SPECIAL APPLICATIONS

Mohammad Mustafa Ghafurian<sup>1\*</sup>, and Brian Elmegaard<sup>1</sup>, Peter Weinberger<sup>2</sup>, Ahmad Arabkoohsar<sup>1</sup>

<sup>1</sup>Department of Civil and Mechanical Engineering Thermal Energy, Lyngby, Copenhagen, Denmark

<sup>2</sup>Institute of Applied Synthetic Chemistry, TU Wien, Getreidemarkt 9/163-01-3, A-1060 Vienna, Austria

\*Corresponding Author: mmug@dtu.dk

### ABSTRACT

Heat pipes are highly efficient and passive heat transfer mechanisms widely used in engineering systems. Their compact design, easy installation, and low maintenance make them popular across various equipment types, even in remote locations. While copper is commonly chosen for its high thermal conductivity, it may not be suitable for certain environments like humid spaces (e.g., geothermal and seawater areas) or places with strong electric and magnetic fields (e.g., transformers). Therefore, this study aims to analyze alternative materials such as aluminum, titanium, steel, nickel, and ceramics for heat pipes numerically. Specifically, it will conduct a comparative analysis of different wick types associated with these materials, evaluating their thermal and fluidic performance using water as the working fluid. Additionally, economic assessments will be carried out to understand the cost implications of these materials compared to copper. The results show that the temperature difference between the evaporator and condenser regions for various materials: Copper, Steel AISI 4340, Ceramics, Aluminum, Titanium, and Nickel are, respectively, 0.04, 0.26, 0.04, 0.06, 1.29, and 0.16 degrees Celsius. Therefore, the worst performance occurs with titanium due to its low thermal conductivity.

### 1 INTRODUCTION

The heat pipes are capable of efficiently and compactly removing a significant amount of heat from various engineering systems, including electronic components (Shafahi et al., 2010). These devices are usually made of copper, which is considered weak in terms of corrosion resistance. It is important to pay attention to material compatibility with their applications. To this purpose, Lee et al. manufactured a series of tabular heat pipes made of stainless steel, intended for low-grade heat recovery applications in a corrosive exhaust environment (Lee et al., 2017). They presented the fabrication process, the systems used for testing thermal performance, and the modeling. Their experimental findings indicated that the ratio of water filling significantly influences the thermal performance of heat pipes. Also, a numerical model was created, and its predictions were found to be reliable when compared with experimental data. The model suggested that selecting a material with a higher coefficient of thermal conductivity could enhance the thermal performance of the heat pipe. However, this must be balanced against thermal performance and application considerations such as corrosion.

In another study, a laser-powered bed fusion (LPBF) additive manufacturing (AM) method to build titanium-ammonia heat pipes with incorporated micro-scale lattice capillary wick structures was employed (Moon et al., 2020). The technology used a combination of laser parameter optimization trials and experimentation with capillary lift height to enable the reduction of the size of the lattice structure cell to below the then-existing state-of-the-art processes. This resulted in the ability to achieve a degree of capillary pumping against gravity, while still meeting the requirement of 30 W direct thermal management for a simulated microprocessor. The AM heat pipe technology was the first of its kind. The paper provided an overview of the technology and compared it to a stainless steel, ammonia heat

pipe, with a screen mesh capillary wick structure, that had been developed concurrently with the AM heat pipe.

Wuttijumnong et al. developed and evaluated a high-performance capillary pump for use in loop heat pipes that could transfer 500 W of heat over a distance of 250 mm (Wuttijumnong et al., 2012). The wick structure, an essential part of the loop heat pipe, offered the necessary capillary pumping, liquid-vapor phase separation, and a heat leak barrier from the evaporation section to the compensation chamber. To create a wick structure with appropriate physical properties, they selected highly pure (> 99.5%) nickel powders with average particle sizes of 2, 10, 12, and 75  $\mu\text{m}$  for a sintering experiment. It found that nickel powder was effectively sintered when maintained at a temperature of 750 – 850  $^{\circ}\text{C}$  for one hour. Among the four nickel powders, the NM-12 powder, with an average particle diameter of 12  $\mu\text{m}$ , provided the most suitable porous structure when sintered at 850  $^{\circ}\text{C}$  for one hour. This structure showed high porosity (> 72%), high permeability ( $> 2 \times 10^{-13} \text{ m}^2$ ), a smaller pore radius (< 7.2  $\mu\text{m}$ ), low shrinkage (< 22%), good axial straightness, and acceptable strength. The paper outlines the primary issues encountered during sintering trials and the corresponding solutions to prevent them. During the sintering experiment, a high-strength, lubricious center rod made from stainless steel with a boron nitride coating was used to replace the carbon rod in order to overcome the problem of removing the center rod. The methodologies developed in the research could be applied to the fabrication of high-performance capillary wicks for miniature to large-scale loop heat pipes.

The use of a heat pipe made of sintered silicon carbide (SSiC) as a ceramic heat pipe was another research for high-temperature heat transfer in a special area (Hack et al., 2017). In this study, a single bench-scale ceramic heat pipe (with a length of 1,070 mm and an outer diameter of 22 mm) with zinc as a working fluid could achieve a performance of over 1,000 W under testing conditions. The optimal performance was achieved using 100g of zinc, which filled approximately 11% of the heat pipe length under liquid conditions. The current operating temperature of the heat pipes on the heating gas side could be tested up to 980  $^{\circ}\text{C}$ , meaning that the temperature inside the heat pipe, which is the same as the boiling temperature of the working fluid, must be slightly lower than this point. The pressure inside the heat pipe was below the ambient pressure at a working fluid temperature of up to 907  $^{\circ}\text{C}$ .

Aluminum is another alternative material that can be used in the challenges of managing heat for the application of electronic devices (Chang et al., 2021). For example, Cheng et al. (Chang et al., 2021) designed and manufactured using 3D printing technology a unique flat heat pipe made of aluminum, featuring micro-grooves. In this study, aluminum powder was selectively melted and solidified to form the shape of the heat pipe. The sintered aluminum powder increased the inner surface roughness of the heat pipe, and the micro-grooves that were designed further amplified the capillary forces induced by the wick structure. The wettability of the working fluid (acetone) was excellent, and the capillary forces were adequate for the working fluid to flow back into the pipe. The study also examined the effects of the working fluid filling ratio on the heat pipe's heat transfer performance. The revealed that the filling ratio of 10% resulted in the best heat transfer performance and the lowest thermal resistance. The 3D-printed flat heat pipe was also tested for managing the heat of an LED. The LED's temperature could be maintained below 40  $^{\circ}\text{C}$ , thereby extending its lifespan.

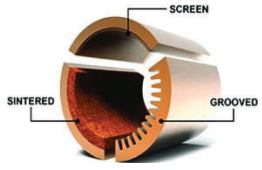
While numerous studies have delved into alternative materials and their performance in different heat pipe configurations, a noticeable research gap persists regarding a comprehensive examination that directly contrasts the efficacy of these materials with other suitable options for heat pipes operating under comparable conditions. Hence, the aim of this study is to conduct a numerical analysis comparing substitute materials for heat pipes and wicks, encompassing copper, aluminum, titanium, steel, nickel, and ceramics. This study aims to compare different types of wicks, namely screen, sintered, and grooved, along with various materials. The study will evaluate their thermal and fluidic performance using water as a working fluid. The comparison will also include the cost estimation of these materials as compared to copper.

## 2 DESCRIPTION

This study investigates three types of wicks, namely screen, sintered, and grooved. The screen wick, characterized by its high permeability, typically ranging from  $10^{-11}$  to  $10^{-12} \text{ m}^2$ , and a concurrently high

porosity, usually within the 40% to 70% range, serves as an effective capillary structure in heat pipes. In contrast, the sintered wick exhibits a moderate to high permeability, falling between  $10^{-11}$  and  $10^{-13}$   $m^2$ , accompanied by a moderate porosity ranging from 30% to 50%. This type of wick is formed through the sintering of fine metal powders, offering a balanced compromise between capillary action and structural integrity. On the other hand, the grooved wick, with a permeability typically considered low to moderate ( $10^{-12}$  to  $10^{-14}$   $m^2$ ) and a corresponding low to moderate porosity of 20% to 40%, utilizes channels or grooves to guide the capillary movement of the working fluid, providing a structured pathway for heat transfer. Each wick type is selected based on specific application requirements, considering factors such as heat pipe size, working fluid properties, and thermal demands for optimal performance. The screen, sintered, and grooved wick structures were considered for numerical modeling and comparison using aluminum, copper, titanium, steel, nickel, and ceramics as the wick materials. Table 1 represents the properties of selected wick structures. To this study, these wicked heat pipes were modeled and characterized in COMSOL software. The modeled heat pipe has three sections: evaporator, adiabatic, and condenser. There are three regions in each section: envelope, wick, and vapor. The evaporator, adiabatic, and condenser are each 100 mm long. The outer diameter, thickness of wick, and envelope are 14mm, 2mm, and 1mm, respectively. For the wick section, laminar flow is used based on Brakeman equations. The evaporator wall is kept at a constant temperature of 383.15 K, and the condenser is assumed to have a convection coefficient of 1200 W/m<sup>2</sup> K. The heat input in this scenario is well below the capillary limit of 7.5 kW. For instance, the CPU of a regular consumer PC generates around 10-100 W. Therefore, the heat pipe operates without any restrictions, and a steady-state solution can be obtained (Sudhan et al., 2022).

**Table 1:** Properties of different wick structures.

Wick type	Average pore diameter( $\mu m$ )	Porosity (-)	Permeability ( $m^2$ )	Shape
Screen (Sireesha et al., 2023)	19.1	$\approx 0.7$	$3.15 \times 10^{-11}$	
Sintered (Grissa et al., 2018)	8.3	$\approx 0.55$	$1.17 \times 10^{-12}$	
Grooved (Sudhan et al., 2022)	A groove width of 0.4 mm and a depth of 2 mm	$\approx 0.4$	$9.99 \times 10^{-12}$	

### 3 GOVERNING EQUATION

The equations used for the modeling are described in this section. The mass and momentum conservation equations for flow are given as follows (Zhu & Vafai, 1999).

Steam region

$$\frac{\partial u_v}{\partial x} + \frac{\partial v_v}{\partial r} + \frac{v_v}{r} = 0 \tag{1}$$

$$\rho_v \left( u_v \frac{\partial u_v}{\partial x} + \frac{\partial u_v}{\partial r} \right) = -\frac{\partial p_v}{\partial x} + \mu_v \left( \frac{\partial^2 u_v}{\partial r^2} + \frac{1}{r} \frac{\partial u_v}{\partial r} \right) \tag{2}$$

$$\frac{\partial p_v}{\partial r} = 0 \tag{3}$$

Water region

$$\tag{4}$$

$$\frac{\partial u_l}{\partial x} + \frac{1}{r} \frac{\partial}{\partial r} (ru_l) = 0$$

$$\frac{\mu_l}{\varepsilon} \left( \frac{\partial^2 u_l}{\partial r^2} + \frac{1}{r} \frac{\partial u_l}{\partial r} \right) - \frac{\mu_l}{K} u_l - \frac{\rho_l F \varepsilon}{K^{1/2}} |u_l| u_l - \frac{\partial p_l}{\partial x} = 0 \quad (5)$$

where  $e$ ,  $K$ , and  $F$ , are respectively porosity, permeability, and a geometric function based on the porous wick structure detailed in (Vafai, 1984). The temperature profile of the wall is determined under the assumption that the wall temperature is consistent across the condenser and evaporator sections. A model of heat conduction is employed for the wall and the liquid-wick area. Consequently, the temperature profile of the heat pipe can be depicted in the following manner.

$$T_{\text{wall}}(x) = \begin{cases} T_b + \frac{Q}{2\pi L_c} \left[ \left( \frac{\ln\left(\frac{R_o}{k_w}\right)}{k_{\text{wall}}} + \frac{\ln\left(\frac{R_w}{R_v}\right)}{k_{\text{eff}}} \right) \left( 1 + \frac{L_c}{L_e} \right) + \frac{1}{hR_o} \right] & 0 \leq x \leq L_e \\ T_b + \frac{Q}{2\pi L_c} \left( \frac{\ln\left(\frac{R_o}{k_w}\right)}{k_{\text{wall}}} + \frac{\ln\left(\frac{R_w}{R_v}\right)}{k_{\text{eff}}} + \frac{1}{hR_o} \right) & L_e \leq x \leq L_e + L_a \\ T_b + \frac{Q}{2\pi L_c h R_o} & L_e + L_a \leq x \leq L \end{cases} \quad (6)$$

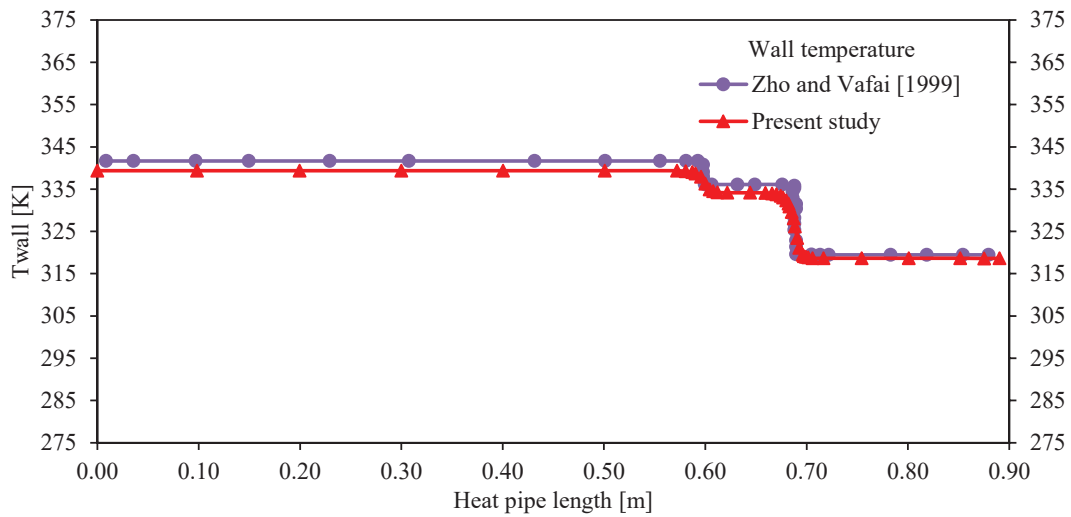
Where  $k_{\text{wall}}$  represents the thermal conductivity of the heat pipe wall, and  $k_{\text{eff}}$  denotes the effective thermal conductivity of the wick saturated with liquid. The operation of the condenser in a steady state can be depicted as:

$$Q_c = 2\pi R_o L_c h (T_{\text{wall},c} - T_b) \quad (7)$$

Where  $R_o$  is the outer radius of the heat pipe,  $L_c$  is the length of the condenser section,  $h$  is the outside convective heat transfer coefficient,  $T_{\text{wall},c}$  is the wall temperature at the condenser section, and  $T_b$  is the bulk temperature of the coolant.

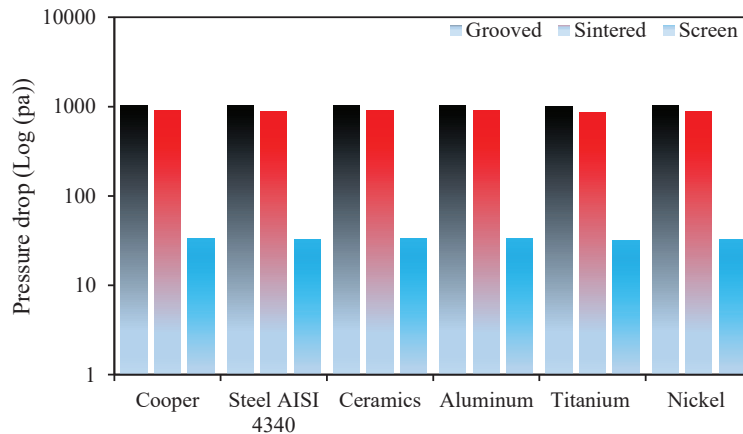
#### 4 RESULTS AND DISCUSSION

The validation results for wall temperature are given in Figure 1. For this purpose, the physical dimensions of the heat pipe were  $R_o=9.55$  mm,  $R_w=9.4$  mm,  $R_v=8.65$  mm,  $L_e=60$  cm,  $L_a=9$  cm, and  $L_c=20$  cm, based on the dimensions used in Ref (Zhu & Vafai, 1999). The effective pore radius, porosity, and permeability of the wick were selected as 54 mm, 0.9, and  $1.5 \times 10^{-9}$  m<sup>2</sup>, respectively. Also, the input heat flux considered was 455 W. The temperature profile of the wall, as predicted in this study, aligns seamlessly with the analytical solution provided by (Zhu & Vafai, 1999), indicating a robust agreement between the present work and established theoretical insights. For the modeling in the present study, the Brakeman module in COMSOL Multiphysics was used compared to the Darcy method used in the validation data (Zhu & Vafai, 1999). Due to the exclusive consideration of vertical velocity vectors in the Darcy approach, our findings exhibit slight discrepancies.



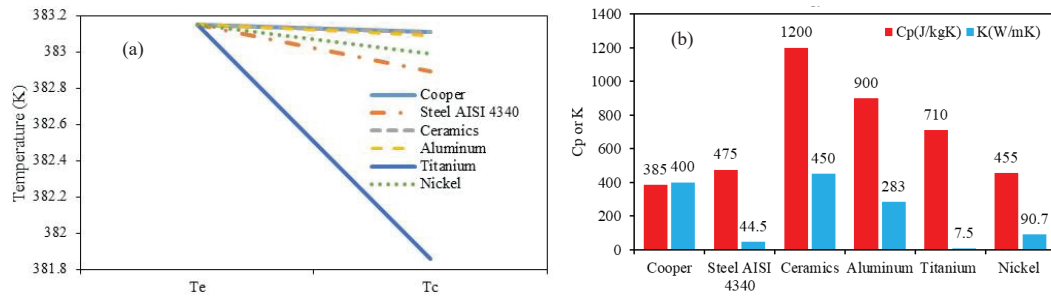
**Figure 1:** The temperature profile of the wall for validation.

Figure 2 compares pressure drops for grooved, sintered, and screen wicks made of copper, aluminum, titanium, steel, nickel, and ceramics. As illustrated in all cases, the screen wick has the lowest pressure drop while the lower pressure drop is observed in the sintered wick than in the grooved wick. In general, a lower porosity increases the pressure difference between evaporator and condenser sections as the fluid flows harder within the pipe (please see Table 1).



**Figure 2:** Pressure drop comparison for various copper wicks.

The temperature change from the evaporator to the condenser chambers is compared in Figure 3 for various materials with the screen wick as the best candidate. The temperature of evaporator chambers ( $T_e$ ) is fixed at 383.15 K in all cases. Among the cases, the titanium results in the most severe temperature difference compared to others. It reaches a condenser temperature ( $T_c$ ) of 381.86 K when using a screen wick (see Figure 3 (a)). A lower conductivity brings about higher temperature differences. Since titanium has the lowest conductivity (see Figure 3 (b)), it shows the highest temperature difference in all types of wicks. Aluminum, copper, and ceramics performed identically in all cases. They both achieved a roughly 0.05 K change between  $T_e$  to  $T_c$ . Nickel achieved a  $T_c$  of 383 K. Steel (AISI 4340) performed similarly to nickel so that, it gives a  $T_c$  of 382.89 K. All in all, it could be concluded that copper, aluminum, and ceramics are the best materials in terms of thermal performance.



**Figure 3:** (a) Temperature drop comparison for various materials used in screen wick. (b) comparison of heat conductivity ( $K$ ) and capacity ( $C_p$ ) coefficients for various materials.

Table 2 presents the price per kilogram and applications of diverse materials. Notably, steel emerges as the most cost-effective option. Consequently, the utilization of steel heat pipes becomes a viable alternative owing to their attributes of high temperature/pressure resistance, corrosion resistance, non-toxicity, safety, and extended lifespan, particularly in scenarios where the temperature differential between the evaporator and condenser regions is not critical. While copper, aluminum, and ceramics exhibit comparable heat transfer performance, copper, despite being frequently the most economical, is susceptible to acidic corrosion and freezing. As a result, aluminum and ceramics present themselves as viable alternatives within similar applications. Ceramics, distinguished by their robust resistance to corrosion, electrical insulating properties, and endurance at elevated temperatures, prove especially suitable in environments with dense electrical and magnetic fields link transformers, despite their inherent fragility. Additionally, nickel exhibits compatibility with alkali metals, commonly can be employed as working fluids in high-temperature heat pipe applications.

**Table 2:** Price of various materials (updated on January 12<sup>th</sup>, 2024) and their applications (Alibaba.com, 2024; Economics, 2024; Made-in-China.com, 2024).

Material	Price (USD/kg)	Applications	Considerations
Steel	0.54	Oil & Gas, petrochemicals, chemical applications	When high durability and low cost are required. For low-grade heat recovery applications in a corrosion exhaust environment (Lee et al., 2017).
Cooper	0.825	Electrical devices	When high formability is required (Narendra Babu & Kamath, 2015)
Aluminum	2.22	off-the-shelf air conditioning/dry cooling such as airplane	When low weight is required (Kuroda et al., 2013; Moon et al., 2020)
Nickel	16.19	Suitability for gravity-opposed operation with potassium as the working fluid	When high formability and durability are required (Hansen et al., 2015)
Titanium	25.75	Desalination and Space Electronic Devices	When low weight and high durability are required (RyanJ. et al., 2020)
Ceramic	0.2-100	Cooling in an oil-immersed transformer, to preheat combustion air or gases, e gasification processes	When electric resistance, high temperatures, and corrosion resistance are required (Ghafurian et al., 2023; Hack et al., 2017)

## 5 CONCLUSIONS

In conclusion, the study conducted a comprehensive numerical analysis of alternative materials for heat pipes, considering their thermal and fluidic performance as well as economic implications. The comparative analysis of different wick types associated with these materials revealed that the screen wick is the best among all due to pressure drop in the wick region. The numerical study revealed that the temperature differences between the evaporator and condenser regions for different materials were as follows: Copper (0.04°C), Steel AISI 4340 (0.26°C), Ceramics (0.04°C), Aluminum (0.06°C), Titanium (1.29°C), and Nickel (0.16°C). Although copper is commonly used due to its high thermal conductivity, it may not be suitable for certain environments. Since copper is sensitive to acidic corrosion and freezing. Aluminum is also acid-sensitive, but it can be used when low weight and high durability are required. Ceramics on the other hand are anti-corrosion, electric resistant, and durable at high temperatures, but ceramics are very fragile. Therefore, the selection of materials for heat pipes should be based on a balance between performance and cost, taking into account the specific environmental conditions.

## NOMENCLATURE

F	Geometrical function
h	Convective heat transfer coefficient [W/m <sup>2</sup> K]
K	Permeability of the wick [m <sup>2</sup> ]
k	Thermal conductivity [W/m K]
L	Length of the heat pipe [m]
P	Pressure [Pa]
Q	Heat [W]
r	Cylindrical coordinates [m]
R	Radius [m]
T	Temperature [K]
u	Horizontal velocity component [m/s]
v	Vertical velocity component [m/s]
x	Cylindrical coordinates [m]
<b>Greek symbols</b>	
$\varepsilon$	Porosity of the wick
$\mu$	Dynamic viscosity [N s/m <sup>2</sup> ]
$\rho$	Density [kg/m <sup>3</sup> ]
<b>Subscripts</b>	
a	Adiabatic
b	Bulk
c	Condenser
e	Evaporator
eff	Effective
l	Liquid phase
o	Heat pipe with pure fluid
v	Vapor
w	Inner pipe wall
wall	Wall

## REFERENCES

- Alibaba.com. (2024). *Titanium Scooter Handle Bar 99.99% Pure Titanium Rod Bars Price Per Kg - Buy Gr5 Titanium Steel Rod, Steel Rods 2mm, Titanium Round Bar Product on Alibaba.com.* [https://www.alibaba.com/product-detail/Titanium-Scooter-Handle-Bar-99-99\\_1600973938989.html?s=p](https://www.alibaba.com/product-detail/Titanium-Scooter-Handle-Bar-99-99_1600973938989.html?s=p)

- Chang, C., Han, Z., He, X., Wang, Z., & Ji, Y. (2021). 3D printed aluminum flat heat pipes with micro grooves for efficient thermal management of high power LEDs. *Scientific Reports*, 11(1), 8255. <https://doi.org/10.1038/s41598-021-87798-4>
- Economics, T. (2024). *Commodities - Live Quote Price Trading Data (tradingeconomics.com)*. <https://tradingeconomics.com/commodities>
- Ghafurian, M. M., Joveini, A., Safarzadeh, S., & Niazmand, H. (2023). Experimental study of passive cooling techniques in an oil-immersed transformer building. *Journal of Thermal Analysis and Calorimetry*, 148(24), 14097-14108. <https://doi.org/10.1007/s10973-023-12693-1>
- Grissa, K., Benselama, A. M., Lataoui, Z., Bertin, Y., & Jemni, A. (2018). Investigations of the thermal performance of a cylindrical wicked heat pipe. *International Journal of Energy Research*, 42(9), 3048-3058. <https://doi.org/https://doi.org/10.1002/er.3973>
- Hack, N., Unz, S., & Beckmann, M. (2017). Ceramic Heat Pipes for High Temperature Application. *Energy Procedia*, 120, 140-148. <https://doi.org/https://doi.org/10.1016/j.egypro.2017.07.147>
- Hansen, G., Næss, E., & Kristjansson, K. (2015). Sintered Nickel Powder Wicks for Flat Vertical Heat Pipes. *Energies*, 8(4), 2337-2357. <https://www.mdpi.com/1996-1073/8/4/2337>
- Kuroda, M., Chang, J.-Y., Gwin, P., Mongia, R. K., Kim, C.-U., Cabusao, G. P., Goto, K., & M.Mochizuki. (2013). *Development of Aluminum-Water Heat Pipe*.
- Lee, H.-M., Tsai, M.-C., Chen, H.-L., & Li, H.-Y. (2017). Stainless Steel Heat Pipe Fabrication, Performance Testing and Modeling. *Energy Procedia*, 105, 4745-4750. <https://doi.org/https://doi.org/10.1016/j.egypro.2017.03.1032>
- Made-in-China.com. (2024). *Ceramic Powder Price, 2024 Ceramic Powder Price Manufacturers & Suppliers | Made-in-China.com*. <https://www.made-in-china.com/products-search/hot-china-products/Ceramic Powder Price.html>
- Moon, S.-H., Choi, K.-S., Lee, J.-H., & Kim, H.-T. (2020). Application of aluminum flat heat pipe for dry cooling near the hot spot of a radar array with a multiscale structure. *Applied Thermal Engineering*, 169, 114894. <https://doi.org/https://doi.org/10.1016/j.applthermaleng.2019.114894>
- Narendra Babu, N., & Kamath, H. c. (2015). Materials used in Heat Pipe. *Materials Today: Proceedings*, 2(4), 1469-1478. <https://doi.org/https://doi.org/10.1016/j.matpr.2015.07.072>
- Ryan J., M., Glen, & Sutcliffe, C. J. (2020). Additive Manufactured Titanium-Ammonia Heat Pipes for Thermal Management of Space Electronic Devices.
- Sireesha, V., Kishore, P. S., & Dharma Rao, V. (2023). Chapter 8 - Advanced wick materials and structures for loop heat pipes. In S. J. Vijay, B. Solomon, & J. Meyer (Eds.), *Materials for Advanced Heat Transfer Systems* (pp. 257-287). Woodhead Publishing. <https://doi.org/https://doi.org/10.1016/B978-0-323-90498-8.00005-1>
- Sudhan, A. L. S., Solomon, A. B., & Sunder, S. (2022). Heat transport limitations and performance enhancement of anodized grooved heat pipes charged with ammonia under gravity and anti-gravity condition. *Applied Thermal Engineering*, 200, 117633. <https://doi.org/https://doi.org/10.1016/j.applthermaleng.2021.117633>
- Vafai, K. (1984). Convective flow and heat transfer in variable-porosity media. *Journal of fluid mechanics*, 147, 233-259.
- Wuttijumnong, V., Singh, R., Mochizuki, M., Goto, K., Thang, N., Tien, N., & Mashiko, K. (2012, 18-22 March 2012). High-performance nickel wick development for loop heat pipes. 2012 28th Annual IEEE Semiconductor Thermal Measurement and Management Symposium (SEMI-THERM),
- Zhu, N., & Vafai, K. (1999). Analysis of cylindrical heat pipes incorporating the effects of liquid–vapor coupling and non-Darcian transport—a closed form solution. *International Journal of Heat and Mass Transfer*, 42(18), 3405-3418.